



PERGAMON

Available online at [www.sciencedirect.com](http://www.sciencedirect.com)

SCIENCE @ DIRECT®

Radiation Physics  
and  
Chemistry

Radiation Physics and Chemistry 68 (2003) 981–994

[www.elsevier.com/locate/radphyschem](http://www.elsevier.com/locate/radphyschem)

# Dose response and post-irradiation characteristics of the Sunna 535-nm photo-fluorescent film dosimeter

M.K. Murphy<sup>a,\*</sup>, A. Kovács<sup>b</sup>, S.D. Miller<sup>c</sup>, W.L. McLaughlin<sup>d</sup>

<sup>a</sup> Battelle–Pacific Northwest National Laboratory, Richland, WA 99352, USA

<sup>b</sup> Institute of Isotopes and Surface Chemistry, Hungarian Academy of Sciences, H-1525 Budapest, Hungary

<sup>c</sup> Sunna Systems Corporation, Richland, WA 99352, USA

<sup>d</sup> Ionizing Radiation Division, Physics Laboratory, National Institute of Standards and Technology, Gaithersburg, MD 20899, USA

Received 25 July 2002; accepted 9 June 2003

## Abstract

Results of characterization studies on one of the first versions of the Sunna photo-fluorescent dosimeter™ have previously been reported, and the performance of the *red* fluorescence component described. This present paper describes dose response and post-irradiation characteristics of the *green* fluorescence component from the same dosimeter film (*Sunna Model γ*), which is manufactured using the injection molding technique. This production method may supply batch sizes on the order of 1 million dosimeter film elements while maintaining a signal precision ( $1\sigma$ ) on the order of  $\pm 1\%$  without the need to correct for variability of film thickness. The dosimeter is a  $1\text{ cm} \times 3\text{ cm}$  polymeric film of 0.5-mm thickness that emits green fluorescence at intensities increasing almost linearly with dose. The data presented include dose response, post-irradiation growth, heat treatment, dosimeter aging, dose rate dependence, energy dependence, dose fractionation, variation of response within a batch, and the stability of the fluorimeter response. The results indicate that, as a routine dosimeter, the green signal provides a broad range of response at food irradiation (0.3–5 kGy), medical sterilization (5–40 kGy), and polymer cross-linking (40–250 kGy) dose levels.

© 2003 Elsevier Ltd. All rights reserved.

**Keywords:** Dosimetry; Film dosimeters; Food irradiation; Radiation processing; Sterilization

## 1. Introduction

Imperfections (lattice vacancies) are produced by ionizing radiation within the ionic lattice of alkali-halide compounds, such as lithium fluoride (LiF), and they act as traps for electrons and electron holes (Schulman, 1979). These defects are known as *color centers* because of their role in the imperfect compound's ability to absorb and re-release energy in the form of visible light photons of characteristic wavelengths (Kaufman and Clark, 1963). The process of latent photon emission from a solid or liquid phosphor material after being supplied with a certain form of energy is called *luminescence*. Inducing color-center

luminescence using excitation by light is referred to as optically stimulated luminescence (OSL), and is the mechanism utilized for the subject dosimeter. Because this process does not involve the separation of the electron from its original ion—and the time-consuming path through the conduction band—the luminescence is considered a fluorescence event (Becker, 1969; Kröger, 1948).

The various types of color centers existing within the ionic lattice of an alkali-halide-based dosimeter can be revealed by the various absorption peaks in the absorption spectrum of the material. One of the main optical absorption bands revealed is the M-band, and this band was selected for dosimetry because the color centers associated with it produce the largest luminescence signals at room temperature and above. For LiF, the M-band is centered at 442 nm, and is the result of

\*Corresponding author. Fax: +1-509-376-1992.

E-mail address: [mk.murphy@pnl.gov](mailto:mk.murphy@pnl.gov) (M.K. Murphy).

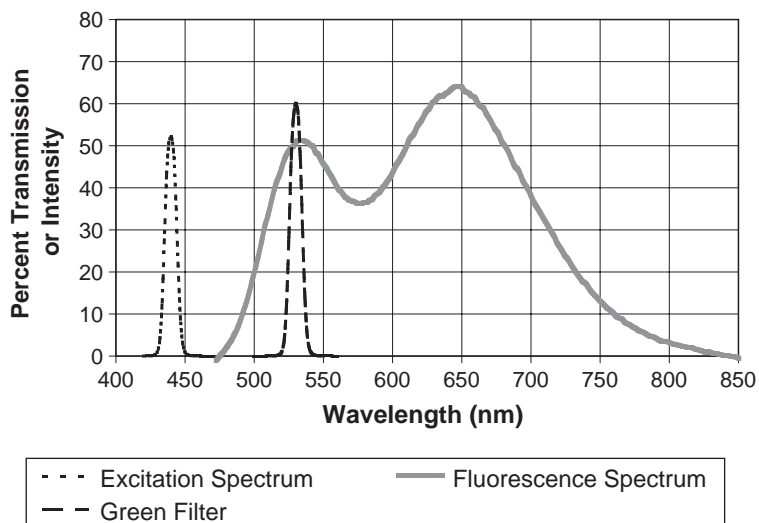


Fig. 1. The excitation spectrum and resulting fluorescence spectrum emitted from the Sunna Model  $\gamma$  dosimeter, along with the transmission curve for the green emission filter.

several types of color centers; thus, 442-nm excitation light will produce luminescence emission peaks at several different wavelengths (see Fig. 1). This characteristic behavior results in excitation and emission spectra with essentially no overlap. Therefore, by using broad-band optical filtration, this M-center luminescence can be measured with a visible-light photosensitive system without interference from the excitation light. This readout process is a non-destructive one; that is, the dosimeter can be read multiple times without significantly altering the signal (Murphy et al., 2003). Because the population of M-centers grows almost linearly with increasing radiation dose, M-center luminescence provides a viable method for use in radiation dosimetry (McLaughlin et al., 1979; Miller and Endres, 1990; Miller, 1996).

The present work describes the methods and results of dose response and post-irradiation measurements performed using the 535-nm emission (from now on referred to as *green* emission) from batch 0399-20 of the *Sunna Model*  $\gamma$  dosimeter.<sup>1</sup> This dosimeter is a 1 cm  $\times$  3 cm polymeric film of 0.5-mm thickness containing a microcrystalline dispersion of LiF. Studies include dose response, post-irradiation growth, dosimeter aging, energy dependence, dose rate dependence, dose fractionation effects, variation of response within a batch, and the stability of the fluorimeter response. Data for both food irradiation and sterilization dose levels are presented. Murphy et al. (2003) report on the environmental effects for the same model dosimeter. Kovács et al. (1999, 2000, 2002) and McLaughlin et al. (1999a, b)

describe the response characteristics of the *red* fluorescence component of earlier versions of the Sunna dosimeter.

## 2. Experimental

All variables associated with each experiment were controlled to ensure that the data reveal the true nature of the parameter being investigated. The estimated combined uncertainty of the dosimeter system used for the experiments was evaluated so as to be able to recognize the limitations of the experiments and to properly interpret the measurement data. Except during readout, all the test dosimeters utilized were kept in light-tight packaging. Unless otherwise indicated, all the dosimeter readouts were performed in a room with lights that were covered with yellow filters to filter out UV and blue wavelengths that are known to influence the signal of freshly irradiated dosimeters (Murphy et al., 2003). All dosimeter readout results were provided in terms of net signal; that is, the irradiated dosimeter reading minus the mean reading of a random sample of unirradiated dosimeters. This relatively small signal from an unirradiated dosimeter is due to the fluorescence from the materials within the dosimeter.

### 2.1. Readout instrument

A Model TD-700 fluorimeter, manufactured by Turner Designs,<sup>2</sup> was used for measuring the fluorescent

<sup>1</sup>Sunna Systems Corporation, Richland, WA.

<sup>2</sup>Turner Designs, Sunnyvale, CA.

signal from the irradiated dosimeter. The TD-700 consists of a 440-nm blue light source (a blue LED array and a 440-nm optical interference filter) for the excitation light, a sample chamber with a green (530 nm) optical interference filter to transmit the desired fluorescence wavelength band, and a green-sensitive photo-multiplier tube (PMT) to measure the fluorescence photons. The bandwidths associated with the excitation and emission filters are 10 nm. The area of the dosimeter that is both “excited” and “read” is  $0.33 \text{ cm}^2$ . The unit displays a digital readout in fluorimeter signal units (fsu), which are proportional to the PMT current. The sensitivity of the fluorimeter response is easily adjusted by the user—each sensitivity setting allowing a  $60X$  factor in absorbed dose range.

Other fluorimeters might be used, for example the Model FR-2141 fluorimeter,<sup>3</sup> with optical filtration to pass the green emission from the Sunna dosimeter.

### 2.2. Fluorimeter response stability

The spectrofluorimetric response variation for the TD-700 instrument was monitored using a solid fluorescent standard Model 7000-994, also supplied by Turner Designs, which fluoresces in the green. Additional data obtained during the long-term post-irradiation stability study show the emission from this solid fluorescent standard to be consistent to within at least  $\pm 2\%$  ( $1\sigma$ ) over a 5-month period. The solid standard was placed in the fluorimeter chamber periodically over a period of 13 days and the fluorimeter reading was recorded each time. The standard deviation of the readings was then calculated for both short and long periods. It was assumed that any observed variation in the OSL signal was due to the LEDs and/or PMT instabilities.

### 2.3. Spectra

The fluorescence spectra from irradiated dosimeters were measured using a Perkin-Elmer Model LS50B luminescence spectrophotometer,<sup>4</sup> and the optical transmission curves were generated using a Perkin-Elmer Model Lambda-6 spectrophotometer.

### 2.4. Variation of response of dosimeters

In the present study, even though the injection mold used contained four separate dosimeter cavities, dosimeters made from each separate cavity within the injection mold were still considered to be from the same batch. To measure the variation of response within dosimeters from a single cavity, 30 dosimeters were randomly selected from cavity #1 and were simulta-

neously irradiated to 5 kGy with gamma radiation in the calibrated Pacific Northwest National Laboratory (PNNL)  $^{60}\text{Co}$  field (MDS Nordion Model GB650 irradiator). To measure the variation of response between dosimeters from different cavities, 20 dosimeters randomly selected from each of the four cavities were also irradiated to 5 kGy. The dose distribution in the volume containing the dosimeters during irradiation was estimated to be uniform within 0.5%.

### 2.5. Dose response

Dose response data were obtained from dosimeter samples irradiated with  $^{60}\text{Co}$  gamma radiation at PNNL and at the Institute of Isotopes and Surface Chemistry (IISC) of the Hungary Academy of Sciences. The absorbed dose rate of the  $^{60}\text{Co}$  field at PNNL is measured using a calibrated ionization chamber (ICRU 14 method (ICRU, 1969)). For PNNL irradiations, the Sunna dosimeters were surrounded by 4.5 mm of PMMA to achieve charge-particle equilibrium (CPE). Dose response data were also obtained from dosimeter samples irradiated with 4.5-MeV E-beam at a commercial radiation processing facility. The absorbed dose of the E-beam was measured using Far West radiochromic film, which was co-located with the Sunna film. The dosimeters were covered with 25 mm styrofoam to try and achieve electron equilibrium. The useful absorbed dose ranges using the various fluorimeters were established from these data. For some dosimeter sets a post-irradiation heat treatment ( $68^\circ\text{C}$  for 15 min) was performed at 10 min after irradiation; those not treated were read out 24 h after irradiation. The heat treatment protocol is used if dosimeter signal stabilization is needed soon after dose (see Heat Treatment).

### 2.6. Post-irradiation stability—short term

For the short-term stability study, sets of dosimeters were irradiated at PNNL with  $^{60}\text{Co}$  gamma radiation to doses of 0.2, 0.4, 0.6, 1.0, and 4.0 kGy (using Model GB650 irradiator at 4.5–14 kGy/h), a set was irradiated at a commercial gamma facility to 20 kGy, and a set was irradiated at a commercial E-beam facility to 35 kGy. Reading out of these dosimeters began immediately after the end of irradiation, and continued at periodic intervals until each set was stabilized. The irradiation temperatures were  $24\text{--}29^\circ\text{C}$  for the PNNL irradiations, approximately  $38^\circ\text{C}$  for the commercial gamma facility irradiations, and approximately  $24^\circ\text{C}$  for the commercial E-beam irradiations. The storage temperature for all facilities was in the range of  $22\text{--}24^\circ\text{C}$ , and each dosimeter was read only once so that the signal growth effect of multiple readouts did not influence the results (see Results section).

<sup>3</sup>Sensolab Ltd., Göd, Hungary.

<sup>4</sup>Perkin-Elmer Corporation, Norwalk, CT.

This procedure was also performed for dosimeters irradiated at PNNL and stored at 0°C and dose levels of 0.6, 1.0, and 5.0 kGy to determine the influence of temperature on the time taken to reach a permanent fluorescent signal.

### 2.7. Post-irradiation stability—long term

Due to the lack of historical data on the long-term consistency of the solid fluorescence standard used (Turner Designs Model 7000 series),<sup>1</sup> we did not depend on it as a reference for the Sunna dosimeter's long-term stability study. Therefore, although the reading of the solid fluorescence standard was recorded at the time each set of dosimeters was read, this fluorescence standard reading was not used to correct dosimeter readings.

The test was accomplished by irradiating sets of dosimeters (using PNNL's GB650 <sup>60</sup>Co irradiator) to a consistent dose on a frequency of approximately every 1–2 months, and then reading out all of the sets together at the end of the study. In this way it was possible to track the long-term stability of the dosimeters, with the only variable being the repeatability of the dose delivered (which is known to be within about 0.4%). If the readout from a specific set of dosimeters at month 1, for example, was significantly different from a readout of the same set at month 6, the difference would be due to a combination of pre-irradiation aging of the dosimeter batch and post-irradiation transformation of color centers over time. The dosimeters were not heat treated after irradiation. Also, the dosimeters were not stored under tightly controlled environmental conditions, but were stored in the PNNL laboratory where typical conditions are approximately 21–24°C and 20–60% relative humidity.

### 2.8. Dosimeter aging

Any change in the irradiated dosimeter's emission over long periods, as would be revealed in the long-term stability study described above, would be the result of both pre-irradiation aging of the dosimeter batch and post-irradiation color center transformation over time. Therefore, the maximum possible effect due to pre-irradiation aging could be determined.

### 2.9. Post-irradiation heat treatment

Heat treatment studies were performed after irradiation using a calibrated NEY Model 160A muffin convection laboratory oven,<sup>5</sup> as well as a Lindberg/Blue Model MO1420-1 mechanical convection laboratory oven.<sup>6</sup> Studies were performed to determine: (1) the

optimum heat treatment temperature, (2) the optimum heat treatment duration, (3) the optimum time after irradiation to perform the heat treatment, (4) if the effect of heat treatment was influenced by the absorbed dose value of the dosimeter and (5) how the amount of storage time before heat treatment influenced the final stabilized signal.

### 2.10. Energy dependence

To generate calculated energy-dependence curves, the photon mass-energy-absorption coefficients (MEACs) and the electron mass-collision-stopping-power coefficients (MCSPs) for LiF were obtained from published tables (Hubbell and Seltzer, 1995) for the energy range of 0.01–10 MeV, and referenced to the MEACs and MCSPs for water. It was determined that the density–thickness of the Sunna film corresponded to the range of approximately 0.25-MeV electrons; therefore, for gamma irradiation the MEAC curve would be valid for energies lower than approximately 0.25 MeV, and the MCSP curve would be valid for energies somewhat greater than this. The MEACs are valid when most of the dose is due to electrons created *inside* the dosimeter, and the MCSPs are valid when most of the dose is due to electrons created *outside* the dosimeter. These MEAC and MCSP curves are only valid for situations where CPE conditions exist.

Measured data were obtained by irradiating films to PNNL's X-ray beams of known average energies (35, 53, 73, 100, 120 keV), as well as PNNL's <sup>137</sup>Cs (662 keV) and <sup>60</sup>Co (1250 keV) beams. All absorbed dose rates were traceable to NIST via ICRU 14 (ICRU, 1969) and ICRU 17 (ICRU, 1970) protocols. To minimize the uncertainty in the delivered absorbed dose, the amount of buildup material used during the Sunna film irradiations was made consistent with the wall thickness of the ionization chamber used to calibrate the associated beam. The uncertainty in the delivered absorbed dose was calculated to be 2.5% at the 95% confidence level.

### 2.11. Dose rate dependence

Dosimeter responses at different absorbed dose rates were obtained from dosimeter samples irradiated with <sup>60</sup>Co gamma radiation at PNNL and 4.5-MeV electrons at a commercial E-beam facility. Dosimeters were read out 24 h after irradiation, with no heat treatment performed. See the Dose response section for the methods used to measure the absorbed doses for the gamma and E-beam fields.

### 2.12. Dose fractionation

Dose fractionation effects for the scenario of a refrigerated irradiation facility processing chicken was

<sup>5</sup>The J.M. NEY Company, Bloomfield, CT.

<sup>6</sup>Lindberg/Blue Inc., Asheville, NC.

evaluated by summing the dose from three separate passes through a gamma-ray irradiation cell at 1 kGy per pass (i.e., 3 kGy total). Testing was performed for dosimeters maintained at 0°C during and after irradiation. The absorbed dose rate was 15.3 kGy/h. Various sets of six dosimeters were irradiated to 3 kGy, 1 kGy at a time, and in the exact same geometry. The only difference in the various sets was the duration of time between each 1-kGy irradiation, which varied from 0 to 61 min. For each set of dosimeters, 10 min after the third 1 kGy irradiation, three of the dosimeters were placed in the oven and treated for 15 min at 68°C, and the remaining three dosimeters were read out at 24 h without heat treatment.

Dose fractionation testing for a third scenario involved summing the dose from *two* separate passes through a gamma-ray irradiation cell at 1 kGy per pass (i.e., 2 kGy total) at an irradiation and storage temperature of 23°C. Plotting the mean net dosimeter response versus the time duration between 1-kGy runs provides useful dose fractionation information for both heat-treated and non-heat-treated dosimeters.

### 3. Results and discussion

#### 3.1. Fluorimeter response stability

The variation in the inherent response of the TD-700 over time—without adjusting the sensitivity of the instrument—was measured to be  $\pm 0.2\%$  (one standard deviation) over 24 h. The associated value at approximately 95% confidence level is  $\pm 0.4\%$ . None of the readings are outside the  $2\sigma$  confidence interval. Over a period of 13 days the response variation was measured to be  $\pm 0.4\%$  (one standard deviation), and the associated value at approximately 95% confidence level was  $\pm 0.9\%$ . Again, none of the readings were outside the  $2\sigma$  confidence interval. Therefore, the data suggest that this model of fluorimeter is stable enough over a 2-week period that adjustment is not necessary. In the event that a fluorimeter response *does* eventually drift outside the desired range, the solid fluorescent standard may be used to monitor and reset the instrument.

#### 3.2. Spectra

Fig. 1 shows the excitation spectrum and resulting fluorescence spectra (background subtracted) from a dosimeter irradiated to 20 kGy, along with the transmission curve for a green interference filter of the type used in the TD-700. The figure shows that the fluorescence spectra consist of green and red emission components centered at 535 and 645 nm, respectively. These peaks represent two different types and orientations of color centers.

#### 3.3. Variation of response of dosimeters

The random variation of response of dosimeters made from a single mold cavity was measured to be  $\pm 0.36\%$  at one standard deviation, and 0.73% at the 95% confidence level. Similar testing on pre-conditioned dosimeters (proprietary method) indicates a within-cavity deviation of 0.2% at one standard deviation. The maximum between-cavity deviation of response was measured to be  $\pm 0.8\%$  at one standard deviation. This high precision makes it unnecessary for the user to measure, and correct for, the thickness of individual dosimeters.

#### 3.4. Dose response

Figs. 2 and 3 show the OSL dose response curves for the color centers associated with the green emission for dosimeters irradiated to gamma radiation from  $^{60}\text{Co}$  sources and electron beam. Data are shown for dosimeters both with and without the stabilizing post-irradiation heat treatment. The results indicate, using two fluorimeter sensitivity settings, that a useable dose range of approximately 0.3–150 kGy is possible for gamma and approximately 0.3–250 kGy for E-beam. Each sensitivity setting can support a 60X factor in absorbed dose range. The lowest value within the quoted dose range is still within approximately  $\pm 1.5\%$  precision (one standard deviation). The divergence of the gamma and E-beam curves above 30 kGy (which results in the slightly greater dose range observed for E-beam) could be explained by the greater adiabatic heating of the dosimeter in the E-beam, dose fractionation, incident electrons creating a different type or different ratio of color centers than incident gamma rays, the higher LET of E-beam combined with phosphor impurities, or a combination of these. Data shown in Fig. 4 indicates a maximum 2% difference in response between dosimeters irradiated with gamma radiation ( $^{60}\text{Co}$ ) and electrons (4.5-MeV E-beam) in the 7–30 kGy range shown.

The overall uncertainty associated with measuring absorbed dose using the Sunna dosimeter was obtained at several radiation processing facilities, and was found to be in the range of 4.3–4.9% at the 95% confidence level when in situ calibration was performed. The method used to calculate the uncertainties is consistent with international standards (ISO, 1993; ISO/ASTM, 1995).

#### 3.5. Post-irradiation stability—short term

Fig. 5 shows the post-irradiation growth of the green emission from dosimeters irradiated to various doses ranging from 0.6 to 20 kGy using gamma radiation, and dosimeters irradiated to 35 kGy using E-beam. All dosimeters were stored at room temperature

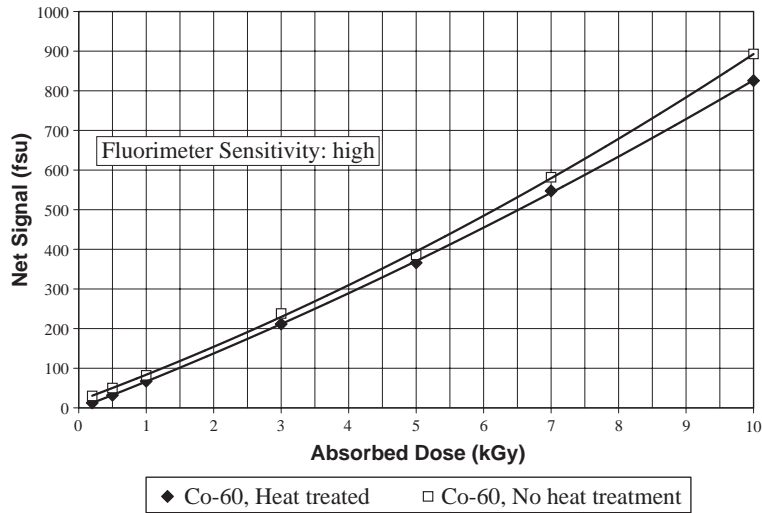


Fig. 2. Dose response of the Sunna Model  $\gamma$  dosimeter’s green emission at low doses using  $^{60}\text{Co}$  gamma radiation at 3.9 kGy/h. Heat treatments were performed 10 min after irradiation, and dosimeters not treated were read out 24 h after irradiation. A Model TD-700 fluorimeter on high sensitivity was used.

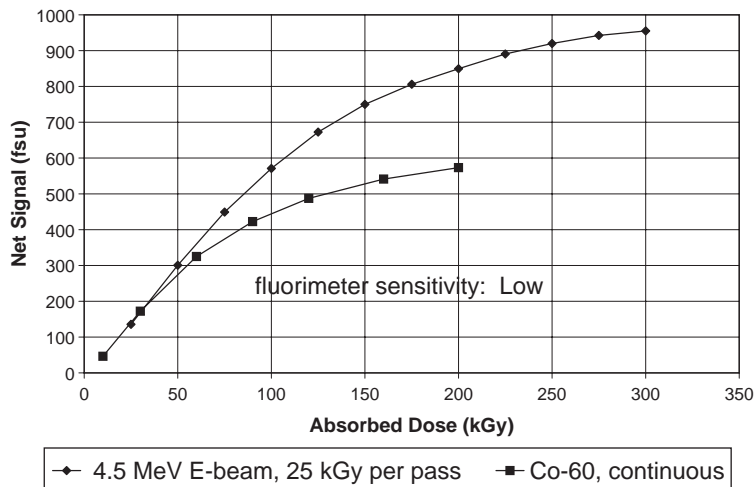


Fig. 3. Dose response of the Sunna Model  $\gamma$  dosimeter’s green emission at high doses using  $^{60}\text{Co}$  gamma radiation and 4.5-MeV electrons. Dosimeters were read out 24 h after irradiation without heat treatment being performed. A Model TD-700 fluorimeter on low-sensitivity setting was used.

conditions (22–24°C). The results indicate that the stabilization time for the green emission is approximately 22 h for gamma-irradiated dosimeters, and is independent of dose in this range. The data also show that dosimeters irradiated with E-beam to 35 kGy exhibit a longer stabilization time of 4 days. The reason for this longer stabilization time is under investigation, and is theorized to be due to the incident electrons creating a different type or different ratio of color centers than incident gamma rays, the higher LET of E-beam being more effective

at ionizing phosphor impurities, or a combination of these.

Fig. 6 shows the influence of irradiation and storage temperature on the post-irradiation growth of dosimeters irradiated to 2 kGy. The data indicate that decreasing the irradiation and storage temperature to 0°C increases the time needed for the full stabilization of the green emission from 22 h to 4 days.

When using the green emission for applications that require dose information within the 22-h stabilization period, one can readout the dosimeters at approximately

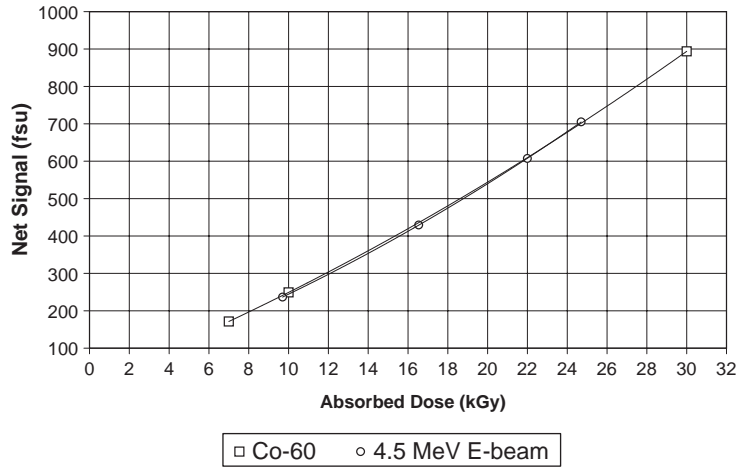


Fig. 4.  $^{60}\text{Co}$  versus 4.5-MeV electron dose response of the Sunna Model  $\gamma$  dosimeter's green emission. No post-irradiation heat treatment was performed, and readout was performed >24 h after irradiation. Indicates same response whether gamma-rays or electrons are used, and that there is no energy effect in the range of 1.25–4.5 MeV.

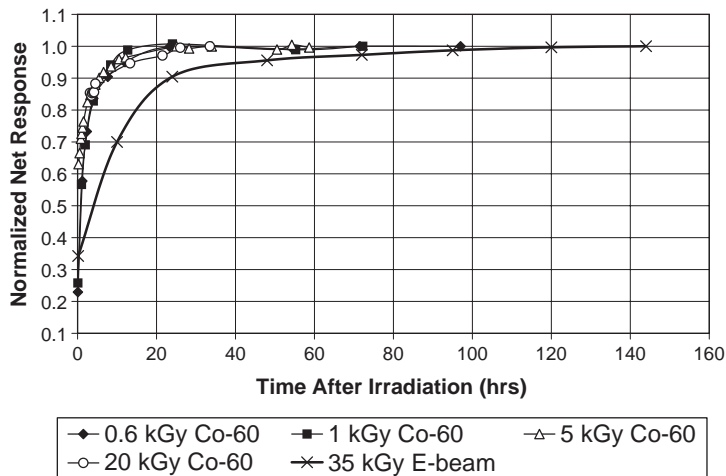


Fig. 5. Influence of absorbed dose level on the post-irradiation stabilization time of the Sunna Model  $\gamma$  dosimeter's green emission using  $^{60}\text{Co}$  gamma radiation at 4.5 to tens of kGy/h. Data are also shown for a commercial E-beam facility at 35 kGy. The data show that the 22-h stabilization time using gamma is independent of absorbed dose level, and that the stabilization time for E-beam irradiated films at 35 kGy is 4 days.

the same time after irradiation for both calibration and routine use, or perform a post-irradiation heat treatment to accelerate the stabilization period (see Heat treatment).

The data show that the slopes for the growth curve in the first hour after irradiation is approximately 1%/min at dose levels of <2 kGy. For doses above this level the slopes improve to between 0.1 and 0.5%/min. Therefore, when using the green emission for routine dosimetry applications where the dose information is needed within the first hour after irradiation (and heat treatment is not performed), the time after irradiation that readout is performed should be within approximately

1 min of when the calibration set was read out for dose levels <2 kGy, and to within a few minutes of when the calibration set was read out for dose levels >2 kGy. This would ensure the errors associated with reading out dosimeters before stabilization do not exceed 1% at one standard deviation.

### 3.6. Post-irradiation stability—long term, and dosimeter aging

Fig. 7 shows the change in signal of an irradiated dosimeter over time, combined with the effects of dosimeter age on the dosimeter response, for dosimeters

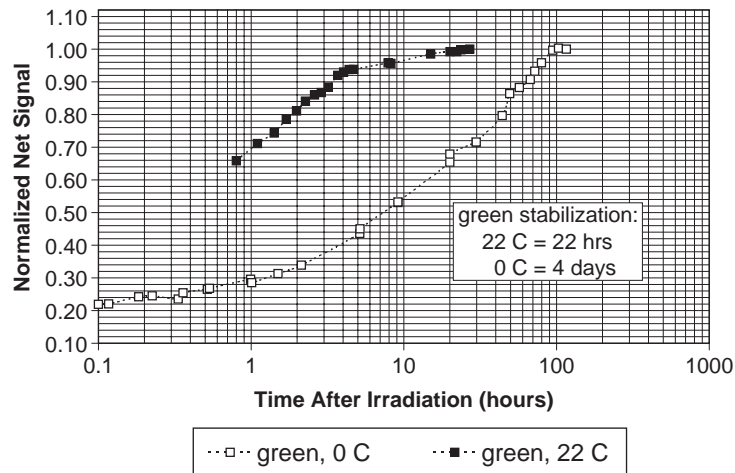


Fig. 6. Influence of irradiation and storage temperatures on the post-irradiation stabilization time of the Sunna Model  $\gamma$  dosimeter's green emission. Irradiations were performed at 2 kGy using  $^{60}\text{Co}$  gamma radiation at 14 kGy/h. The data show that the stabilization time for green emission is dependent on temperature—the lower the temperature the longer the stabilization time.

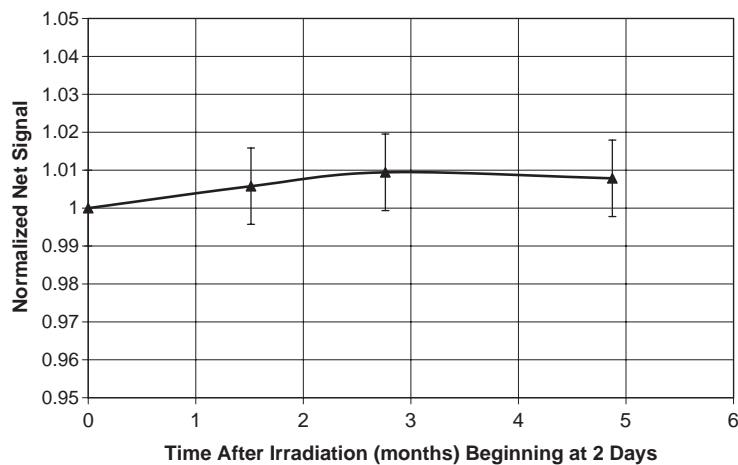


Fig. 7. The effects of batch age on the dosimeter response, combined with the change in emission from an irradiated dosimeter, over long time periods. Results are shown for dosimeters irradiated to 30 kGy.

irradiated to 30 kGy and stored at normal laboratory conditions (approximately 21–24°C and 20–60% relative humidity). The data suggest that these combined effects result in a maximum of approximately 1% change over 5 months for the green emissions. Results of humidity effect studies reported by Murphy et al. (2003) indicate that any increase in batch dose response over time (batch aging effects) or slow long-term growth of irradiated dosimeters are likely due to water absorption. Therefore, dosimeter batch pre-irradiation aging or long-term post-irradiation growth may be controlled by storing dosimeters in a controlled humidity environment.

### 3.7. Heat treatment

Treating the irradiated dosimeters with heat for a relatively short-time duration after irradiation results in accelerating and stabilizing the growth of the dosimeter's green color centers. The effect is to speed up the increase of the number of green color centers formed. Fig. 8 shows the influence of various heat-treatment temperatures, applied for 20 min, upon the green emissions of the dosimeter. From these data, the optimum treatment temperature was determined to be approximately 70°C. Additional testing showed that the minimum heating duration needed to stop the inherent

growth was approximately 15 min in a forced-air oven, and that heating longer than this (tested up to 3 h) did not affect the signal. However, the results also indicated that the dosimeter required additional heating (a minimum duration of 25–30 min) to provide *full* protection from alteration of the emission signal due to exposure to the fluorimeter light. Because this alteration of signal is small, the expanded heating duration is relevant only in cases where dosimeters are archived for potential re-analysis at a future date.

When heat treatment is performed, the value for the final stable emission signal from the dosimeter is dependent on the time after irradiation that the treatment begins, i.e., the treatment does not increase the emission signal to the same stable value that is obtained without treatment. Figs. 9–11 show this heat-treated response versus post-irradiation storage time for various dose levels, storage temperatures, and radiation types. Fig. 9 shows this heat-treated response for the green emission from dosimeters irradiated with gamma rays at PNNL's  $^{60}\text{Co}$  research irradiator to dose levels of 0.4–3 kGy. The dosimeters irradiated at  $0^\circ\text{C}$  were also stored at  $0^\circ\text{C}$ , and those irradiated at  $26^\circ\text{C}$  were stored at  $22^\circ\text{C}$ . The figure provides information on the optimum time for heat treatment to begin (referred to as a Treatment Window), helping to minimize errors in the measured dose. Specifically, the figure indicates that (1) for dosimeters irradiated at temperatures close to room temperature, and stored at approximately room temperature, the slopes of the heat-treatment curves range from approximately 0.3–0.5%/min in the first couple of hours after irradiation, and (2) for dosimeters stored at refrigerated temperatures, the slopes are negligible.

Fig. 10 shows the heat-treated response for the green emission for dosimeters irradiated with electron beam at a large commercial E-beam facility (4.5 MeV) at dose levels of 9.6 and 24 kGy, and at a storage temperature of  $22^\circ\text{C}$ . Because of adiabatic heating of approximately  $0.25^\circ\text{C}/\text{kGy}$ , these dosimeters reach approximately  $26^\circ\text{C}$  and  $30^\circ\text{C}$ , respectively; however, they quickly return to ambient temperature because of the small heat capacity of the films. The results indicate that, for dosimeters maintained at elevated temperatures for short-time periods and stored at approximately room temperature, the slopes of the heat-treatment curves range from approximately 0.05% to 0.4%/min in the first couple of hours after irradiation.

Fig. 11 shows the heat-treated response for the green emission for dosimeters irradiated in a large commercial  $^{60}\text{Co}$  facility at a dose level of approximately 20 kGy, and at a storage temperature of approximately  $22^\circ\text{C}$ . It should be noted that the associated irradiation temperature was approximately  $38^\circ\text{C}$ , and that the dosimeters were at elevated temperatures for an extended period because of the time it takes for product carriers to immerse from the irradiation cells. As with many commercial gamma facilities, due to the time for carriers to exit the maze and delayed accessibility to the carriers, the heat treatment did not begin for these dosimeters until approximately 3 h after final irradiation. Therefore, the data results indicate that, for dosimeters irradiated at elevated temperatures for a relatively long time period and stored at approximately room temperature, the slope of the heat-treatment curve is approximately 0.12%/h from approximately 3–24 h after irradiation. The inclusion of the inherent growth (no heat treatment) curve in Fig. 11 shows the effect of heat

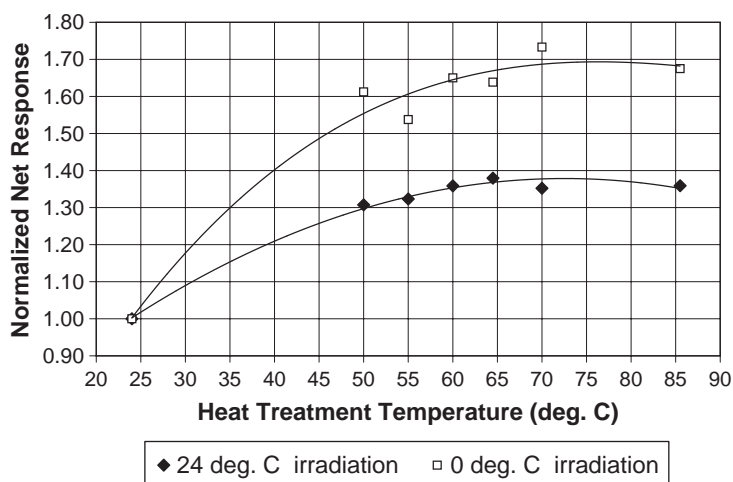


Fig. 8. Influence of oven temperature on the post-irradiation heat-treatment process of the Sunna Model  $\gamma$  dosimeter for both refrigerated and room-temperature irradiations. Results are shown for the green emission from dosimeters irradiated to 2 kGy using  $^{60}\text{Co}$  gamma rays at 14 kGy/h, and heated for 20 min duration. The data indicate that the optimum oven temperature for the green emission is approximately  $70^\circ\text{C}$ .

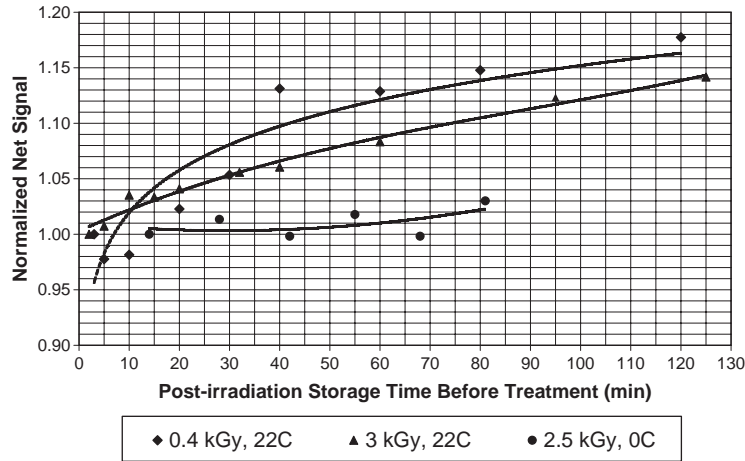


Fig. 9. Influence of heat-treatment start time on the final stable value of the Sunna Model  $\gamma$  dosimeter's green emission for both refrigerated and room temperature irradiations. Results are shown for dosimeters irradiated to 0.4, 2.5, and 3 Gy using  $^{60}\text{Co}$  gamma radiation at 14 kGy/h, and heat-treated at 68°C for 20-min duration.

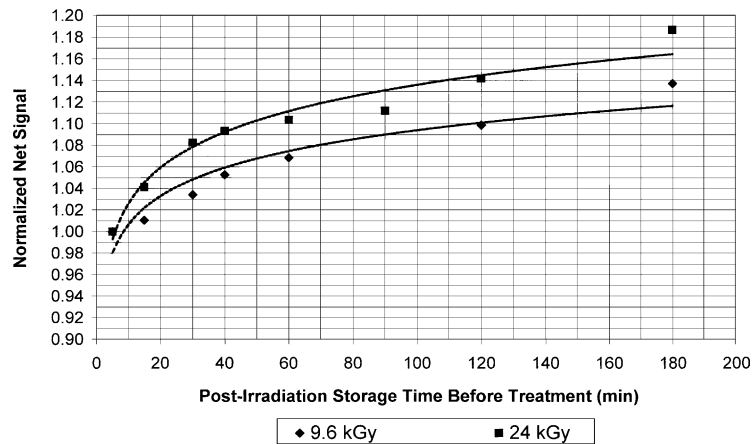


Fig. 10. Influence of heat-treatment start time on the final stable value of the Sunna Model  $\gamma$  dosimeter's green emission for irradiations in a 4.5-MeV commercial E-beam facility. Irradiation temperatures were in the range of 25–30°C. Results are shown for 9.6 kGy (9.6 mA and 6.2 m/min conveyor speed) and 24 kGy (20 mA and 5.2 m/min conveyor speed).

treatment on the irradiated dosimeter's signal over the inherent growth period, relative to the final stable value of the non-treated dosimeters.

### 3.8. Energy dependence

Fig. 12 shows both the calculated and measured energy dependence of the Sunna dosimeter. The difference seen between the calculated and measured data is attributed mostly to a significant change in the relative luminescence efficiency of the LiF at the lower energies (Pradhan, 2003). The data indicate negligible energy dependence in the 0.2–10-MeV range, and a significant effect that peaks at 90 keV at approximately 20% (relative to  $^{60}\text{Co}$  energy).

### 3.9. Dose rate dependence

Dose rate dependence results are shown in Figs. 13 and 14 for various dose levels and dose rate ranges. Fig. 13 shows results for gamma rays at a relatively low dose rate range of 1.6–14.8 kGy/h and dose levels 1, 20, and 40 kGy. For the 1 kGy level, the figure indicates a maximum of approximately +3.5% enhancement of response from 1.6 to 3.9 kGy/h, and that the effect is negligible from 3.9 to 14.8 kGy/h. For the 20 and 40 kGy levels, the figure shows a maximum of approximately –2.8% effect in that range with increasing dose rate.

Fig. 14 shows dose rate effects for high dose and high dose rate using a 4.5-MeV E-beam. The results, at a dose level of 16 kGy for three electron beam currents, indicate

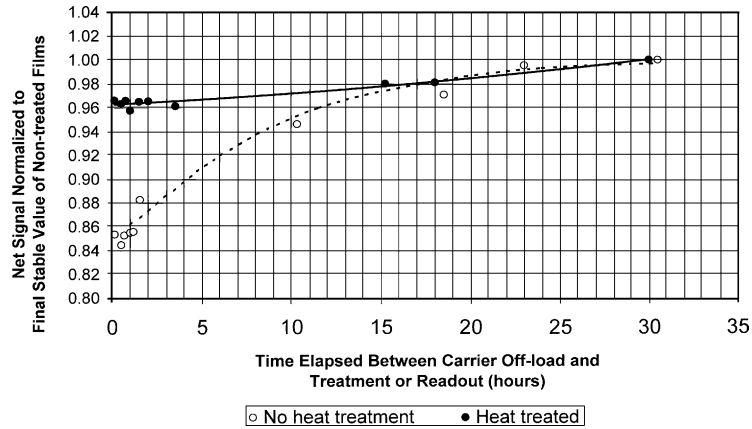


Fig. 11. Influence of heat-treatment start time on the final stable value of the Sunna Model  $\gamma$  dosimeter's green emission for irradiations in a large commercial  $^{60}\text{Co}$  irradiation facility where, due to inaccessibility to the dosimeters, heat treatment could not be performed until about 3 h after irradiation. Absorbed dose value was 20 kGy and the irradiation temperature was 38°C.

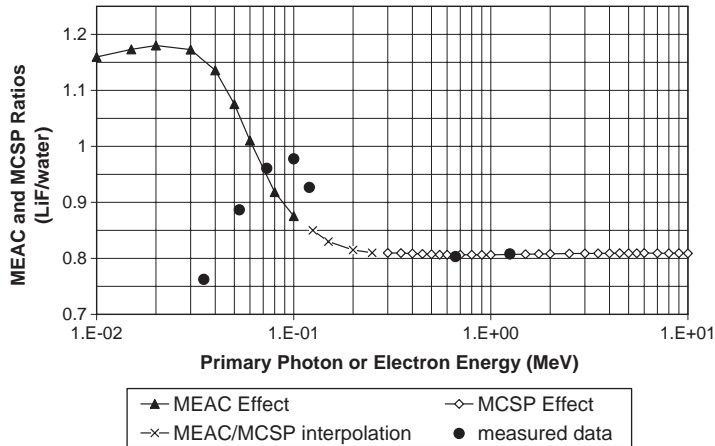


Fig. 12. Calculated and measured energy dependence of the Sunna dosimeter in the range of 10 keV–10 MeV. The difference in the lower energies is attributed mostly to the relative efficiency in color center formation, and perhaps efficiency in luminescence.

a maximum of  $-2.5\%$  change in response from 13 to 33 mA (4.9–12.8 m/min corresponding conveyor speed). The associated dose rates are in the hundreds of kilogray per minute.

### 3.10. Dose fractionation

Dose fractionation results are shown in Figs. 15 and 16 with and without the post-irradiation heat treatment. Fig. 15 shows results for a three-pass scenario of 1 kGy per pass when the dosimeters are irradiated at 0°C, as well as for a two-pass scenario of 1 kGy per pass when the dosimeters are irradiated at 23°C. The results for 3 kGy at refrigerated temperatures show that, for heat-treated dosimeters, there is no measurable fractionation effect for wait periods of  $\leq 30$  min ( $<1\%$ ), and after the

wait period passes 30 min the fractionation effect starts to appear—maximizing at about 7% at 46 min. For dosimeters that are not heat treated, the fractionation effect appears to be a maximum of approximately 5% for wait periods of  $<22$  min, but severe if greater than this.

The results for 2 kGy at room temperature show that, for heat-treated dosimeters, the fractionation effect maximizes at approximately 1.5% for wait periods of approximately 50–60 min.

Fig. 16 shows the results from two separate studies for a two-pass scenario of 25 kGy per pass: one study for heat-treated and one for non-heat-treated dosimeters. The results indicate that, for heat-treated dosimeters, the fractionation effect ranges from 0% to 7% for associated wait times of 0–130 min between passes. For

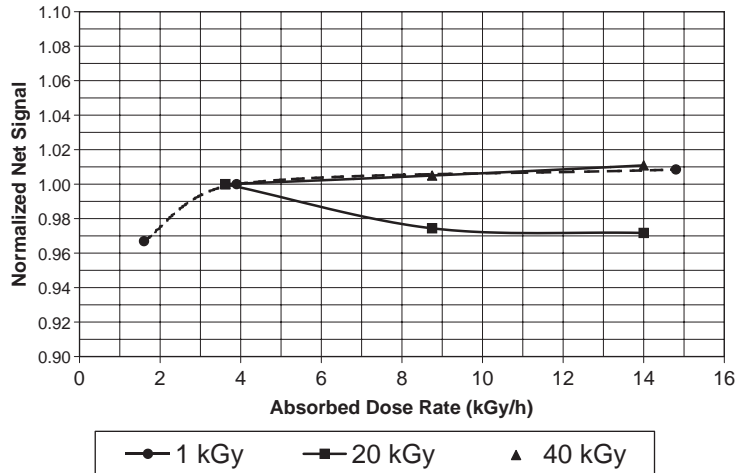


Fig. 13. Dose rate dependence of the Sunna Model  $\gamma$  dosimeter's green emission at a relatively low dose rate range (1.6–14.8 kGy/h) and  $^{60}\text{Co}$  dose levels of 1, 20, and 40 kGy. No post-irradiation heat treatment was performed, and readout was performed 24 h after irradiation.

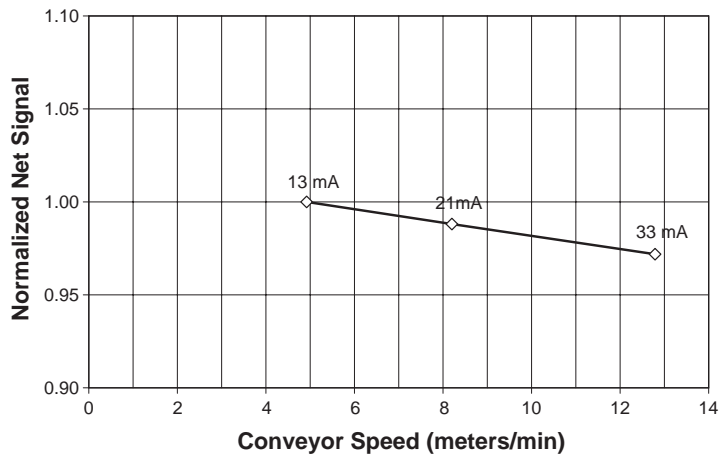


Fig. 14. Dose rate dependence of the Sunna Model  $\gamma$  dosimeter's green emission at a relatively high dose rate range (13–33 mA beam current) and high absorbed dose (17 kGy) using 4.5-MeV electrons. No post-irradiation heat treatment was performed, and readout was performed >24 h after irradiation.

non-treated dosimeters the results indicate a maximum fractionation effect of 2% for a wait time between passes ranging from 0 to 60 min.

#### 4. Conclusions

Evaluations of the green wavelengths of the *Sunna Model*  $\gamma$  dosimeter indicate that it can be used for food irradiation at doses above about 0.3 kGy, and for sterilization and cross-linking applications (10–250 kGy). The uncertainty associated with a delivered absorbed dose in a commercial facility, as measured with

this dosimeter, should be within 4.9% at the 95% confidence level. The post-irradiation stabilization period for the dosimeter is of sufficient duration (22 h for gamma and 4 days for 35 kGy E-beam) that many radiation processing facilities would need to follow one of the two possible protocols to ensure short product release times. One has the choice of either: (1) shortening the post-irradiation stabilizing period by heat treating the irradiated dosimeters at 70°C for at least 15–25 min, or (2) accounting for the post-irradiation growth by selecting at least one consistent readout time for the calibration dosimeters and using the same readout time consistently during routine processing. The heat

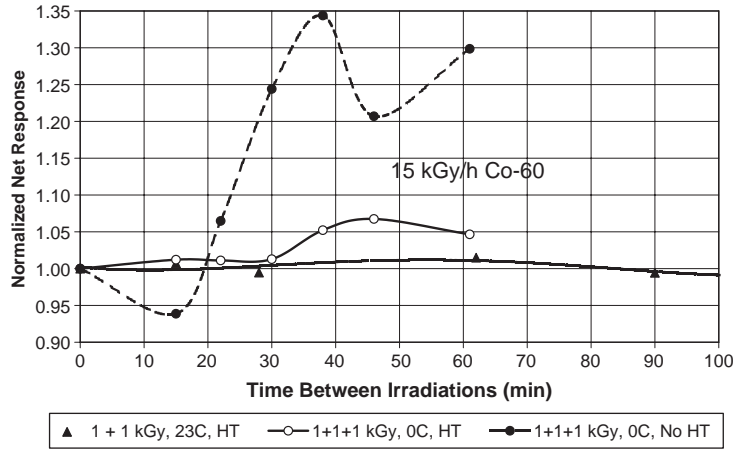


Fig. 15. Dose fractionation effects for the Sunna Model  $\gamma$  dosimeter's green emission for both heat-treated and non-heat-treated dosimeters. Heat treatments were performed 10 min after irradiation, and dosimeters not treated were read out 24 h after irradiation. The two scenarios simulated were three passes of 1 kGy at 15 kGy/h in a refrigerated  $^{60}\text{Co}$  facility, and two passes of 1 kGy at 15 kGy/h in a room-temperature  $^{60}\text{Co}$  facility.

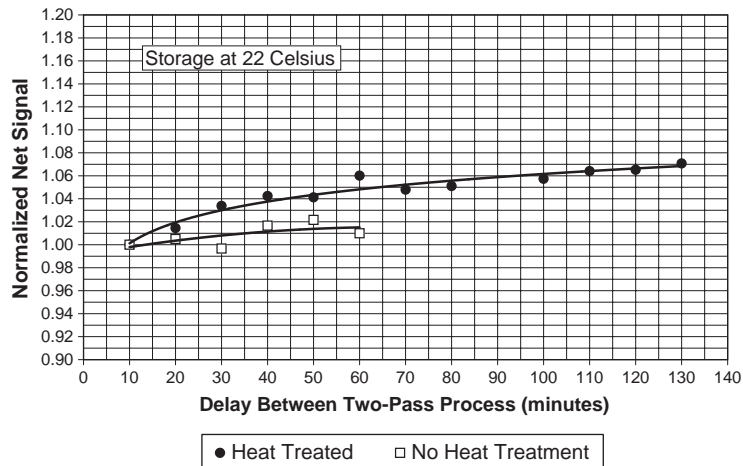


Fig. 16. Dose fractionation effects for the Sunna Model  $\gamma$  dosimeter's green emission for both heat-treated and non-heat-treated dosimeters. Heat treatments were performed 10 min after irradiation, and dosimeters not treated were read out 24 h after irradiation. The protocol was two passes of 25 kGy in a 4.5-MeV E-beam facility.

treatment protocol especially has advantages for dose levels below approximately 1 kGy, and if dosimeters are to be archived for possible future readouts.

The green emission from an irradiated dosimeter stored at normal laboratory conditions is stable over at least 5 months. The pre-irradiation aging effect of a dosimeter batch stored at normal laboratory conditions may be sufficiently negligible that a given calibration could be valid for a year. It may be possible that both of these effects can be controlled by storing dosimeters in a controlled humidity environment.

Other qualities of the dosimeter system are quick readout and robustness, which allow ease of handling,

automated readout mechanisms, and integrity in harsh environments. Because of the injection molding process, batch sizes on the order of 1 million may be possible, while still maintaining high signal precision and with no need to monitor inter-specimen thickness. The system also utilizes inexpensive individual dosimeters and high-quality fluorimeters that have very few components and long lifetimes.

These attributes, along with other attributes reported by Murphy et al. (2003) which indicate the dosimeter's minimal irradiation temperature effects when used in gamma facilities operating in the range of 30–60°C, indicate that the dosimeter system would perform well in

many processing facilities, but especially well in gamma facilities where, due to inaccessibility to the dosimeters, heat treatment is not performed until many hours after irradiation.

## References

- Becker, R.S., 1969. Theory and Interpretation of Fluorescence and Phosphorescence. Wiley, New York.
- Hubbell, J.H., Seltzer, S.M., 1995. Tables of X-ray Mass Attenuation Coefficients and Mass Energy-Absorption Coefficients 1–20 keV for Elements  $Z=1$  to 92 and 48 Additional Substances of Dosimetric Interest, NISTIR 5632. National Institute of Standards and Technology, Gaithersburg, MD.
- ICRU, 1969. Radiation dosimetry: X-rays and gamma rays with maximum photon energies between 0.6 and 50 MeV. International Commission on Radiation Units and Measurements Report 14.
- ICRU, 1970. Radiation dosimetry: X-rays generated at potentials of 5–150 kV. International Commission on Radiation Units and Measurements Report 17.
- ISO, 1993. Guide to the expression of uncertainty in measurement. International Organization for Standardization (ISO), ISBN 92-67-10188-9.
- ISO/ASTM, 1995. Guide for estimating uncertainties in dosimetry for radiation processing. International Organization for Standardization/American Society of Testing and Materials, ISO/ASTM 51707.
- Kaufman, J.V.R., Clark, C.D., 1963. Identification of color centers in lithium fluoride. *J. Chem. Phys.* 38, 1388–1399.
- Kovács, A., Baranyai, M., Wojnarovits, L., Slezsák, I., McLaughlin, W.L., Miller, S.D., Miller, A., Fuochi, P.G., LaValle, M., 1999. A polymeric dosimeter film based on optically stimulated luminescence for dose measurements below 1 kGy. Techniques for high dose dosimetry in industry, agriculture and medicine. Proceedings of the Symposium on IAEA, November 2–5, 1998, Vienna, 1999 (IAEA-SM-356/27), IAEA-TECDOC-1070, pp. 53–58.
- Kovács, A., Baranyai, M., Wojnarovits, L., McLaughlin, W.L., Miller, S.D., Miller, A., Fuochi, P.G., LaValle, M., Slezsák, I., 2000. Application of the Sunna dosimeter film in gamma and electron beam radiation processing. *Radiat. Phys. Chem.* 57, 691–695.
- Kovács, A., Baranyai, M., Wojnarovits, L., Miller, S.D., Murphy, M.K., McLaughlin, W.L., Slezsák, I., 2002. Applicability of the Sunna dosimeter for food irradiation control. *Radiat. Phys. Chem.* 63, 777–780.
- Kröger, F.A., 1948. Some Aspects of the Luminescence of Solids. Elsevier Publishing Co., Inc., New York.
- McLaughlin, W.L., Lucas, A.C., Kaspar, B.M., Miller, A., 1979. Electron and gamma-ray dosimetry using radiation-induced color centers in LiF. *Radiat. Phys. Chem.* 14, 467–480.
- McLaughlin, W.L., Miller, S.D., Saylor, M.C., Kovács, A., Wojnarovits, L., 1999a. A preliminary communication on an inexpensive mass-produced high-dose polymeric dosimeter based on optically stimulated luminescence. *Radiat. Phys. Chem.* 55 (3), 247–253.
- McLaughlin, W.L., Puhl, J.M., Kovács, A., Baranyai, M., Slezsák, I., Saylor, M.C., Saylor, S.A., Miller, S.D., 1999b. Sunna dosimeter: an integrating photoluminescent film and reader system; work in progress. *Radiat. Phys. Chem.* 55 (5–6), 767–772.
- Miller, S.D., 1996. High dose dosimetry using optically stimulated luminescence. *Radiat. Prot. Dosim.* 66, 201–204.
- Miller, S.D., Endres, G.W.R., 1990. Laser-induced optically stimulated M-centre luminescence in LiF. *Radiat. Prot. Dosim.* 33, 59–62.
- Murphy, M.K., Kovács, A., McLaughlin, W.L., Miller, S.D., Puhl, J.M., 2003. The Sunna 535 nm photo-fluorescent film dosimeter response to environmental conditions. *Radiat. Phys. Chem.*, Xref: S0969806X03004432.
- Pradhan, A.S., 2003. Photon energy response of luminescence dosimeters and its impact on assessment of Hp(10) and Hp(0.07) in mixed fields of varying energies of photons and beta radiation. Proceedings of the 13th International Conference on Solid State Dosimetry, 2001, *Radiat. Prot. Dosim.*, in press.

## Further Reading

- Miller, S.D., Murphy, M.K., Kovacs, A., McLaughlin, W.L., Tinker, M.R., 2002. Characteristics and performance of the Sunna high dose dosimeter using green photoluminescence and UV absorption readout methods. *Radiat. Prot. Dosim.* 101(1–4), 53–58.
- Murphy, M.K., 1999. Characterization of a charge-coupled device and lithium-fluoride film imaging system for high-radiation dose applications. Thesis, Washington State University.
- Murphy, M.K., Kovács, A., McLaughlin, W.L., Miller, S.D., 2002. Characterization of a new photo-fluorescent dosimetry system for high-dose applications. *Radiat. Phys. Chem.* 63, 751–754.